

# Solid state preparation and reaction kinetics for Co/B as a catalytic/acidic accelerator for NaBH<sub>4</sub> hydrolysis

Bilge Coşkuner · Aysel Kantürk Figen · Sabriye Pişkin

Received: 14 December 2012 / Accepted: 17 April 2013 / Published online: 1 May 2013  
© Akadémiai Kiadó, Budapest, Hungary 2013

**Abstract** In this study, the solid state synthesis and reaction kinetics for Co/B as a catalytic/acidic accelerator for sodium borohydride (NaBH<sub>4</sub>) hydrolysis were investigated. The Co/B a catalytic/acidic accelerator was synthesized from cobalt(II) chloride hexahydrate (CoCl<sub>2</sub>·6H<sub>2</sub>O) and boron oxide (B<sub>2</sub>O<sub>3</sub>) by a procedure based on solid state synthesis. Differential thermal analyses (DTA) were performed on mixtures of CoCl<sub>2</sub>·6H<sub>2</sub>O and B<sub>2</sub>O<sub>3</sub> at four different heating rates (5, 10, 15 and 20 °C min<sup>-1</sup>) in order to determine the solid state reaction temperatures. Kissinger and Doyle kinetic models were applied to the reaction kinetics data for the solid state preparation. The ideal temperature for the solid-state synthesis of Co/B catalytic/acidic accelerator was 196 °C. Additionally, the catalytic behavior of solid state synthesized Co/B as an catalytic/acidic accelerator for NaBH<sub>4</sub> hydrolysis was investigated. The hydrolysis reactions were performed at temperatures of 22, 40, and 60 °C and the experimental data were fitted to zeroth, first, and second order kinetic models. The maximum hydrogen generation rate was 5,470 ml H<sub>2</sub> min<sup>-1</sup> g<sup>-1</sup> cat and E<sub>a</sub> was only 48.07 kJ mol<sup>-1</sup>.

**Keywords** Hydrogen · Solid State · Kinetics · Sodium borohydride · Hydrolysis · Co/B · Catalytic accelerator · Acidic accelerator

## Introduction

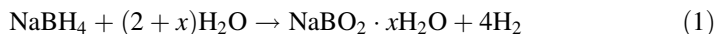
Because it is non-toxic, environmental friendly, widely available and cheap to produce, hydrogen is recognized as competitive alternative to fossil fuels [1]. Hydrogen can be stored as a compressed gas, as a liquid, in a chemical compound (e.g., chemical hydrides or metal hydrides), or physically held within nanoporous structures [2]. For vehicular applications, the U.S. Department of Energy (DOE) has set storage

---

B. Coşkuner · A. Kantürk Figen · S. Pişkin (✉)  
Department of Chemical Engineering, Yıldız Technical University, Istanbul 34210, Turkey  
e-mail: piskin@yildiz.edu.tr; sabriyepisgin@gmail.com

targets; the gravimetric (volumetric) system targets for near-ambient temperature (from 40 to 85 °C) and moderate pressure (less than 100 bar) is 9.0 wt% (81 g l<sup>-1</sup>) for 2015 [3]. Among various hydrogen storage media, chemical hydrides have been regarded as the most promising materials for hydrogen supply and storage due to their capability in supplying ultrapure H<sub>2</sub> and their larger H<sub>2</sub> storage capacity [4, 5].

NaBH<sub>4</sub> is a non-flammable, non-toxic, selective and environmentally friendly light weight complex hydride with high hydrogen capacity (11 wt%). The hydrolysis reaction of NaBH<sub>4</sub> is efficient, generating 4 mol H<sub>2</sub> mol<sup>-1</sup> NaBH<sub>4</sub>. The *x* (mole of water) is generally 2 in the reaction [6–8].



NaBH<sub>4</sub> is self-decomposable in aqueous solution and can be stabilized by alkalization [7, 9].

Co–B catalysts are regarded as optimal catalysts not only due to their high catalytic activity in the hydrolysis of NaBH<sub>4</sub> but also for their low cost. Co–B catalysts have been previously prepared by chemical reduction methods using NaBH<sub>4</sub> as a boron source and also by sol–gel and impregnation methods [10–16]. Metin et al. reported that water-dispersible cobalt(0) nanocluster can be used as a catalyst in hydrogen generation from NaBH<sub>4</sub> and also studied the effect of stabilizer type on activity [17]. Schlesinger et al. reported that NaBH<sub>4</sub> pellets include both acidic and catalytic accelerators that serve to speed up hydrogen generation. Oxalic acid, succinic acid, malonic acid, boric oxide and others were used as acidic accelerators, while metal chloride salts were used as catalytic accelerators [18].

In this study, the solid state preparation of Co/B as a catalytic/acidic accelerator was investigated for the first time. Co/B accelerator as a catalytic/acidic accelerator was prepared from CoCl<sub>2</sub>·6H<sub>2</sub>O and B<sub>2</sub>O<sub>3</sub> as a metal and boron source. Additionally, the kinetics of solid state reactions was investigated using the Kissinger and Doyle kinetic models. Then, the prepared Co/B as a catalytic/acidic accelerator was used in hydrolysis of NaBH<sub>4</sub> for hydrogen generation at 22, 40 and 60 °C under magnetic stirring conditions. The reaction kinetics of hydrogen generation was also investigated.

## Experimental

### Materials

All reagents used in this research were of analytical grade. CoCl<sub>2</sub>·6H<sub>2</sub>O and B<sub>2</sub>O<sub>3</sub> were used as a catalytic and acidic accelerator, respectively. CoCl<sub>2</sub>·6H<sub>2</sub>O (97 %) from Merck, B<sub>2</sub>O<sub>3</sub> (99 %) from Eti Mine Works General Management-Turkey, metallic cobalt powder (≥99.9 %, <150 μ) from Aldrich, NaBH<sub>4</sub> (96 %) from Fluka and sodium hydroxide (NaOH) from Labor Technic were used as received.

### Instrumentation

Crystallinity, morphology, chemical composition and specific surface area of obtained products were performed by using an X-ray diffractometer (XRD), a

scanning electron microscope (SEM), an inductively coupled plasma–optical emission spectrometer (ICP–OES) and Brunauer–Emmett–Teller (BET) analysis. Crystalline structures of solids were determined by the XRD technique. The XRD was carried out at an ambient temperature by using a Philips Analytical X'Pert-Pro diffractometer with Cu  $K_{\alpha}$  radiation ( $\lambda = 0.15418$  nm) at operating parameters of 40 mA and 45 kV with step size  $0.02^{\circ}$  and speed of  $1^{\circ}/\text{min}$ . Phase identification of solids was accomplished using the inorganic crystal structure database (ICSD). The specific surface area of samples was measured using BET (Quantachrome) analysis under  $N_2$  adsorptive gas with multipoint modes. Microstructure studies of the samples were performed using a JEOL (JSM 5410 LV) SEM. The elemental analysis of sample was performed using an ICP–OES (Perkin Elmer, Optima 2100 DV). To prepare samples for analysis, the powder was digested in a hydrochloric acid/nitric acid/hydrofluoric acid/phosphoric acid ( $HCl/HNO_3/HF/H_3PO_4$ ) solution. The samples were analyzed at least three times and mean values were used as one observation.

### Solid state preparation of Co/B as a catalytic/acidic accelerator

The Co/B as a catalytic/acidic accelerator was prepared through solid state methods from the mixture of cobalt and boron sources. Before the solid state synthesis, we determined the temperatures based on DTA analyses. Thermal analysis of samples was performed by use of a Perkin Elmer Diamond instrument, which was calibrated by using the melting points of indium ( $T_m = 156.6$  °C) and tin ( $T_m = 231.9$  °C) under the same conditions as used for the samples.

Two sets of thermal analyses were performed in this study. First, analyses of  $CoCl_2 \cdot 6H_2O$ ,  $B_2O_3$  and reaction mixture ( $CoCl_2 \cdot 6H_2O : B_2O_3 = 1.00 : 1.15$ ) were carried out at a heating rate of  $10$  °C  $\text{min}^{-1}$  in an  $O_2$  atmosphere at a constant flow rate of  $100$  ml  $\text{min}^{-1}$  to  $400$  °C. The samples were placed in standard  $Al_2O_3$  crucibles (Fig. 1a). Reaction mixtures including  $CoCl_2 \cdot 6H_2O$  and  $B_2O_3$  were prepared in a ball milling system in order to obtain a homogeneous mixture. Second, detailed thermal analyses of the reaction mixture were carried out at different heating rates of 5, 10, 15 and  $20$  °C  $\text{min}^{-1}$ . See Fig. 1b for kinetic analyses of solid state synthesis.

Furthermore, to investigate the formation of Co/B as a catalytic/acidic accelerator, the inputs  $CoCl_2 \cdot 6H_2O$  and  $B_2O_3$  were individually heated at  $196$  °C. Fig. 2a, b show the XRD pattern before and after the heat treatment.

After the thermal analyses, the mixture of catalytic and acidic accelerators was settled in  $Al_2O_3$  crucibles (250 ml) and heated in a high temperature calibrated oven at different temperatures, determined from DTA curves, for 4 h to obtain product. Following the solid state reaction, products were kept under inert atmosphere and allowed to cool to room temperature. Before the characterization and hydrolysis tests, catalysts were stored under inert atmosphere.

### Solid state preparations kinetics of Co/B as a catalytic/acidic accelerator

Thermal analysis techniques have been widely used to study the mechanism of solid-state decomposition reactions and a number of non-isothermal kinetic models

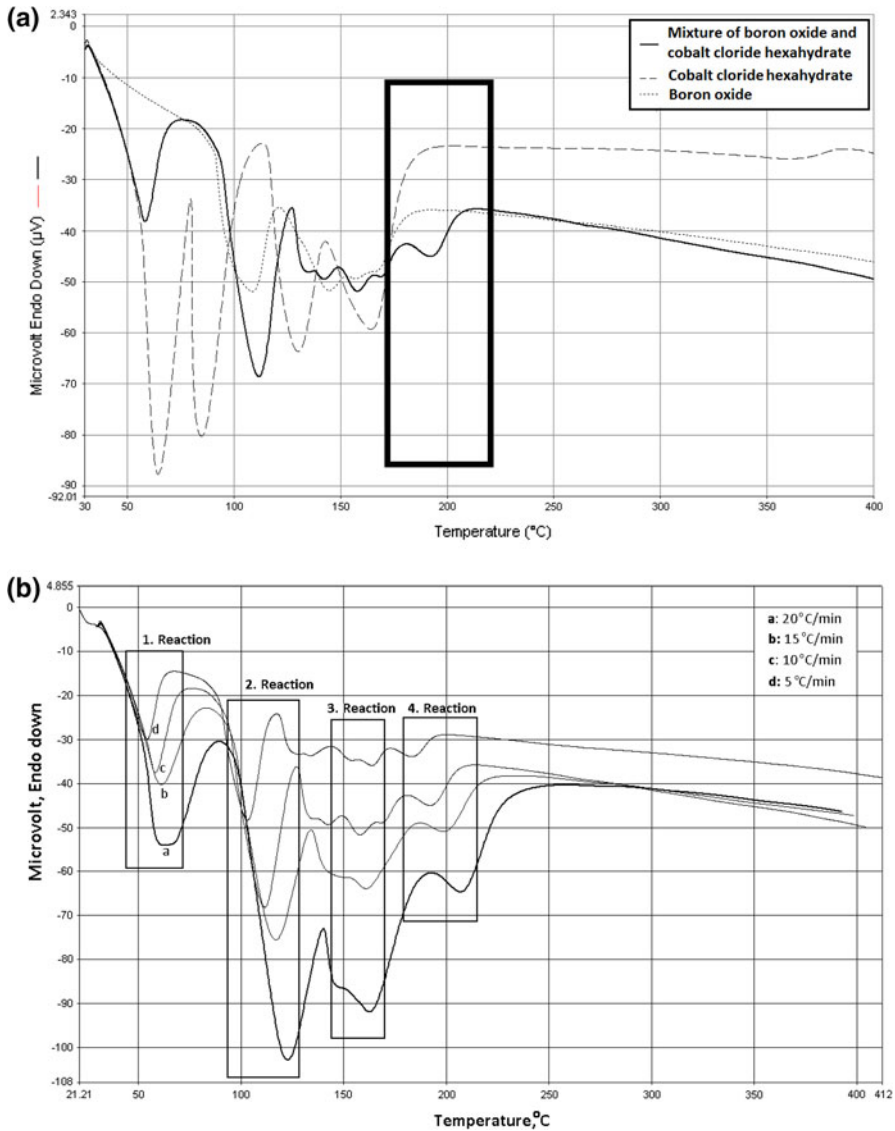


**Fig. 1** DTA curves; **a** reaction mixture and mixture sources at  $10\text{ }^{\circ}\text{C min}^{-1}$  heating rates, **b** reaction mixture at different heating rates

have been developed for calculating the kinetic parameters of the thermal decomposition reactions.

In this study, kinetic analyses of solid state reaction DTA data were performed using the Kissinger and Doyle non-isothermal methods (Fig. 4).

In the Kissinger method [Eq. (2)],  $E_a$  is calculated from a point of the  $T_m$ , which is the temperature at the maximum of the heating derivative mass loss curve for

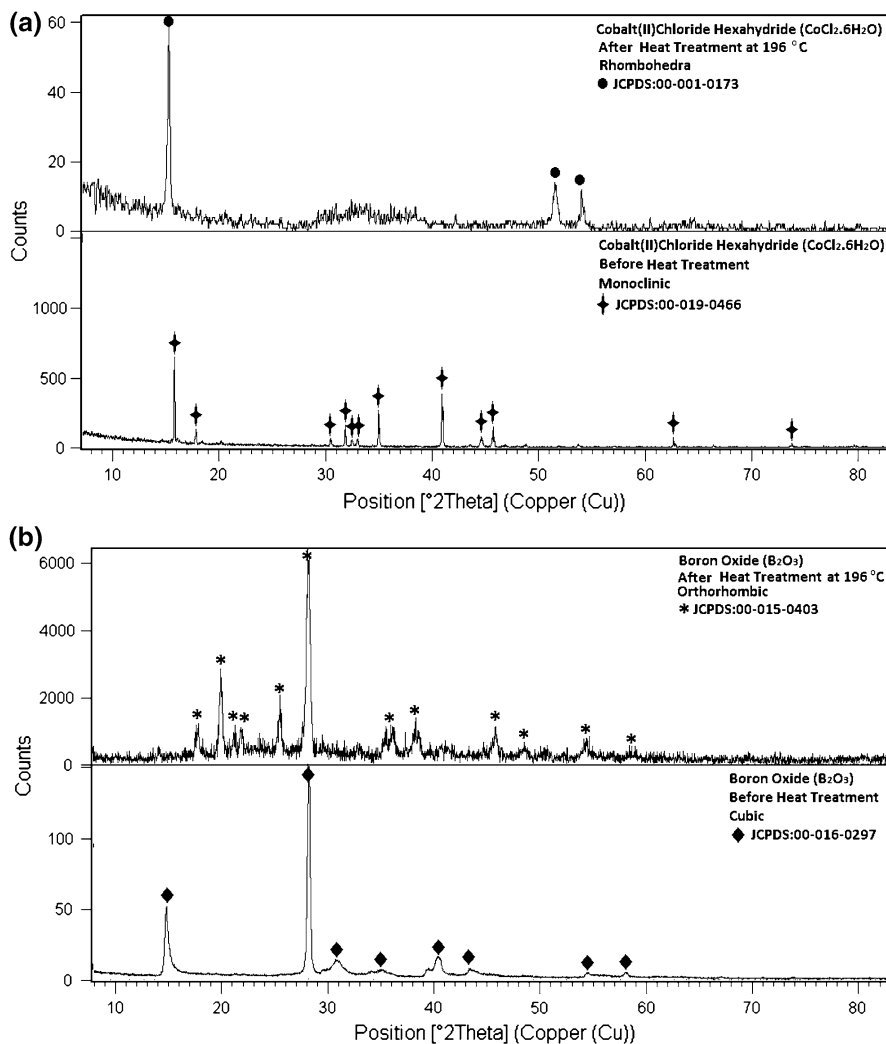


**Fig. 2** XRD patterns of: **a**  $\text{CoCl}_2 \cdot 6\text{H}_2\text{O}$  before and after heat treatment, **b**  $\text{B}_2\text{O}_3$  before and after heat treatment, **c** Solid state products, **d** Co/B catalytic/acidic accelerator

different heating rates.  $E_a$  and  $k_0$  are determined from the slope and the intercept, respectively.

$$\ln \frac{\beta}{T_m^2} = -\frac{E_a}{R} \cdot \left( \frac{1}{T_m} \right) \tag{2}$$

In the Doyle method [Eq. (3)], values of  $\log \beta$  are plotted against  $1/T_m$  giving parallel lines with  $0.4567E_a/R$  slope. The slope of the line gives the  $E_a$  and  $k_0$  and can be calculated from Eq. (4) [17].

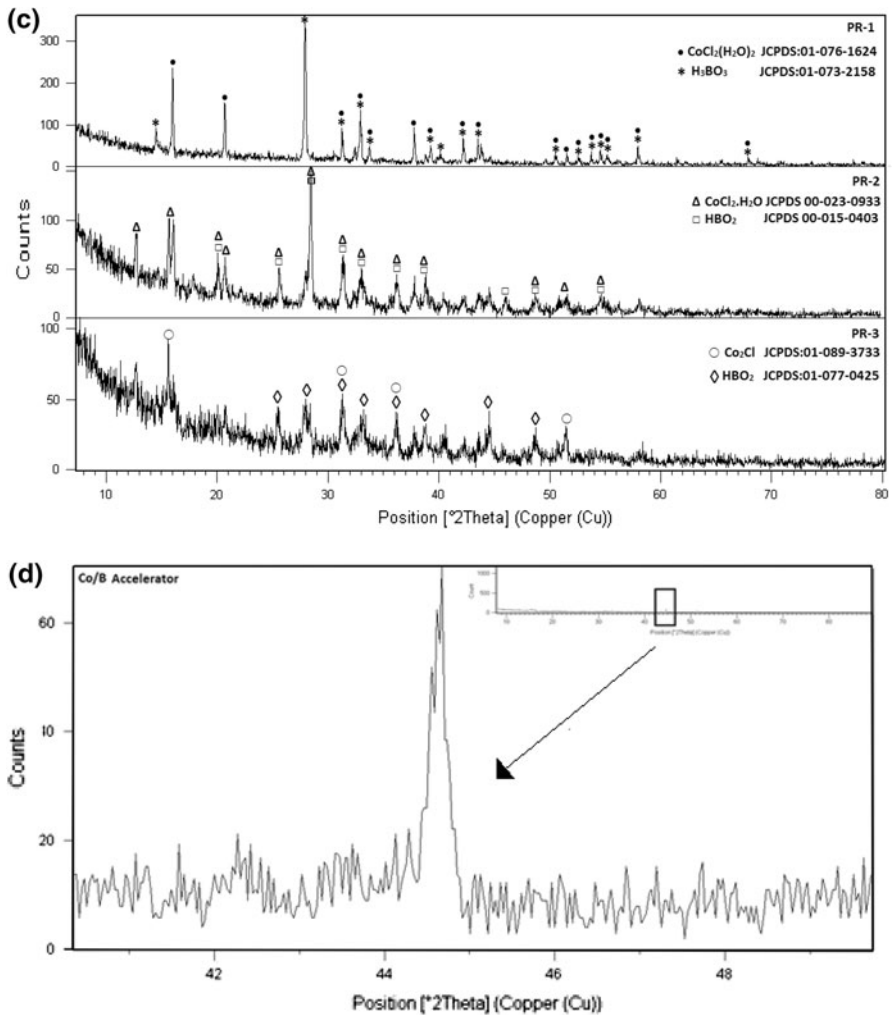


Fig. 2 continued

$$\ln \beta = 0.4567 \cdot \left( \frac{E_a}{RT_m} \right) + \text{Constant} \quad (3)$$

$$k_0 = \exp \left( \frac{E_a}{RT_m} \right) \frac{\beta E_a}{RT_m} \quad (4)$$

Co/B as a catalytic/acidic accelerator for  $\text{NaBH}_4$  hydrolysis

Hydrolysis tests were carried out to determine the hydrogen generation activities of the obtained Co/B catalytic/acidic accelerators from alkali  $\text{NaBH}_4$  solutions. The hydrogen generation tests were performed in a 15 ml hydrolysis glass reactor with

magnetic stirring and a temperature control system. The output of the reactor was connected by rubber tubing to transfer the evolved hydrogen to a water-filled inverted burette in order to measure the generated H<sub>2</sub> volume during the hydrolysis. Alkaline 0.12 M NaBH<sub>4</sub> solutions were prepared with 1 % (wt.) NaOH. 0.0025 g catalyst was used for the hydrolysis test. The hydrogen generation measurement was performed at various temperatures (22, 40 and 60 °C). Hydrogen evaluation time was measured using a chronometer. The hydrolysis glass reactor was kept under magnetic stirring at a frequency of 400 rpm during the hydrolysis. The H<sub>2</sub> production rate was calculated by measuring the volume of the water displaced which was converted into the conversion of NaBH<sub>4</sub> and plotted against the reaction time.

For making comparison, the hydrolysis of NaBH<sub>4</sub> in the presence of 0.0025 g metallic cobalt was carried out at 60 °C under 400 rpm magnetic stirring. Self NaBH<sub>4</sub> hydrolysis without catalyst was also performed under the same conditions in order to show the effect of Co/B accelerator and metallic cobalt on hydrogen generation rate from NaBH<sub>4</sub> (Fig. 5a).

For kinetic modeling, the hydrogen generation rate was converted into reactant (NaBH<sub>4</sub>) concentration as function of time (Fig. 5b). Zeroth, first and second order reaction kinetic models were used for characterizing the kinetic behavior of the hydrolysis of NaBH<sub>4</sub> assisted by Co/B catalyst [5, 18, 19].

The zeroth order kinetic model is seen in Eq. (5), where C<sub>NaBH<sub>4</sub></sub> is the concentration, r is the rate of reaction, k is the reaction rate constant, based on the solution volume:

$$\left( C_{\text{NaBH}_4_0} - C_{\text{NaBH}_4} \right) = -k(T) \cdot t \tag{5}$$

The first order kinetic model is shown in Eq. (6):

$$\ln \left( \frac{C_{\text{NaBH}_4_0}}{C_{\text{NaBH}_4}} \right) = -k(T) \cdot t \tag{6}$$

The second order reaction model is used as seen in Eq. (7):

$$\left( \frac{1}{C_{\text{NaBH}_4}} - \frac{1}{C_{\text{NaBH}_4_0}} \right) = -k(T) \cdot t \tag{7}$$

In all kinetic models, activation energies were calculated from the Arrhenius equation (Fig. 6).

## Results and discussion

### Solid state synthesis of Co/B as a catalytic/acidic accelerator

Fig. 1a shows the DTA curves of CoCl<sub>2</sub>·6H<sub>2</sub>O, B<sub>2</sub>O<sub>3</sub> and mixture of CoCl<sub>2</sub>·6H<sub>2</sub>O and B<sub>2</sub>O<sub>3</sub> at 10 °C min<sup>-1</sup>. The differences between these DTA curves were stated within the enclosed area. The DTA curve of CoCl<sub>2</sub>·6H<sub>2</sub>O consisted of four endothermic peaks at 63, 84, 130 and, 163 °C corresponding to loss of water in the

hydrate structure.  $B_2O_3$  is a stable form that melts at about 400–450 °C. The DTA curve of the mixture illustrates a series of endothermic peaks at 58, 111, 158 and, 193 °C corresponding to the different reactions. These temperatures are quite different from catalytic and acidic materials ( $CoCl_2 \cdot 6H_2O$  and  $B_2O_3$ ). DTA analyses were used to determine the specific temperature values in order to show the interaction between  $CoCl_2 \cdot 6H_2O$  and  $B_2O_3$  compounds. When the three DTA curves were compared, it was clearly seen that the first, second and, third endothermic peaks corresponded to the loss of water in the mixture.  $CoCl_2 \cdot 6H_2O$  was decomposed easily; the dehydration reaction completed before 160 °C. These results suggest that the endothermic peak around 193 °C, which did occur in the DTA curve of  $CoCl_2 \cdot 6H_2O$ , was the interaction between catalytic and acidic accelerators. These results were comparable with XRD analysis results.

Fig. 1b shows the DTA curves of the mixture of  $CoCl_2 \cdot 6H_2O$  and  $B_2O_3$  at different heating rates of 5, 10, 15 and 20 °C  $min^{-1}$ . There were four endothermic peaks in each DTA plot; these peaks corresponded to different solid-state reactions. Taking into consideration each heating rate, the profiles of the DTA curves were indicative of similar behavior. The maximum peak temperatures ( $T_m$ ) of the DTA curves were noted to define the solid-state reaction temperatures (Table 1). It was observed that there were significant differences in the maximum peak temperatures ( $T_m$ ) of the DTA curves. It was therefore best to use the average maximum peak temperature ( $RT_m$ ) for the solid-state synthesis reactions. The  $RT_m$  of solid-state reactions were calculated as 59.54, 113.52, 159.08, and 196.27 °C. At these four temperatures, the reaction powder was heated for 4 h to determine the reaction mechanism of Co/B accelerator synthesis. Depending on increasing of the heating rate both solid state reactions initial and final temperatures were also increased.

Fig. 2a, b show the XRD pattern before and after the heat treatment. When  $CoCl_2 \cdot 6H_2O$  was heated at 196 °C, it released 6 mol of water and transformed into an anhydrous form. According to the XRD results,  $CoCl_2 \cdot 6H_2O$  was defined as monoclinic crystalline phase with  $L2/m$ , 12 space group and number (JCPDS:00-019-0466). After the heat treatment, rhombohedral anhydrous  $CoCl_2$  is observed (JCPDS:00-001-0173) with  $R-3m$ , 166 space group and number.  $B_2O_3$  was identified as cubic structure (JCPDS:00-016-0297), while heated  $B_2O_3$  was defined as orthorhombic  $HBO_2$  (JCPDS:00-015-0403).

As can be seen, when the inputs of the solid state reaction were individually heated at 196 °C crystalline powders were formed, and not amorphous. When the solid state reactions were heated at 196 °C together, they reacted with each other and a new compound with amorphous phase formed. Additionally, Fig. 2b shows

**Table 1** Maximum temperatures of four reaction peaks from DTA curves

Heating rate (°C $min^{-1}$ )	Reaction 1 (°C)	Reaction 2 (°C)	Reaction 3 (°C)	Reaction 4 (°C)
5	53.91	103.11	154.64	183.81
10	58.07	111.64	158.05	193.02
15	62.16	116.76	161.13	200.37
20	64.00	122.56	162.49	207.89
Average	59.54	113.52	159.08	196.27



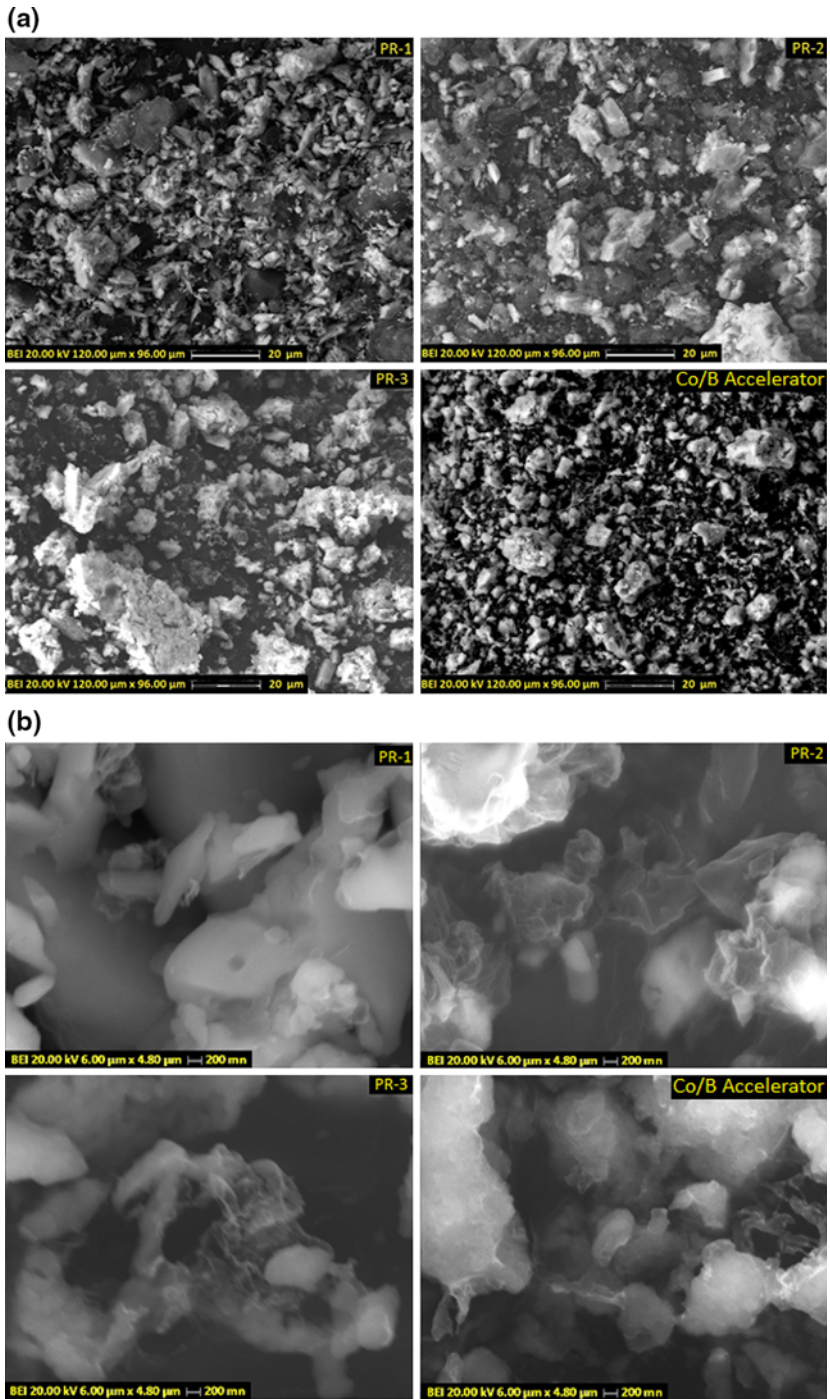


**Fig. 3** SEM image of solid state synthesis products; **a**  $\times 1,000$  magnification, **b**  $\times 20,000$  magnification

that at different heat treatments at 58, 112, 158 °C the products were still crystalline. Based on the XRD results at these lower temperatures, there was no interaction between the inputs.

The product of the first solid state reactions is designated PR-1. According to the XRD analysis results, PR-1 sample included both anorthic structure as  $\text{CoCl}_2(\text{H}_2\text{O})_2$  and  $\text{H}_3\text{BO}_3$  with 01-076-1624 and 01-073-2158 JCPDS files. The characteristic peaks of  $\text{CoCl}_2(\text{H}_2\text{O})_2$  were observed as 16.02°, 20.78° and 32.93° (indexed with ●) and  $\text{H}_3\text{BO}_3$  was observed for the diffraction angles of 14.67°, 14.97° and 28.02° (indexed with \*). The reflection lines were (0 1 0), (1 0 0) and (0 0 2) for  $\text{CoCl}_2(\text{H}_2\text{O})_2$  and (1 1 0), (0 2 0) and (-2 0 1) for  $\text{H}_3\text{BO}_3$ .

The product of the second solid state reactions is designated PR-2. PR-2 had  $\text{CoCl}_2\cdot\text{H}_2\text{O}$  with 00-023-0933 (indexed with  $\Delta$ ) and  $\text{HBO}_2$  with 00-015-0403 (indexed with  $\square$ ) JCPDS file [21].  $\text{CoCl}_2\cdot\text{H}_2\text{O}$  had characteristic peaks at 12.59°, 15.61° and 31.37°. In PR-2,  $\text{HBO}_2$  orthorhombic phase showed characteristic peaks at 20.16°, 25.72° and 28.58°. In this product, with the increasing of the temperature, anorthic structure was changed to orthorhombic structure.

The product of the third solid state reactions is designated PR-3. It had both rhombohedral and orthorhombic structure with two different crystalline structures. The XRD results indicated (0 0 3) as 15.30°, (1 0 1) as 29.45° and (1 0 4) as 35.74° for  $\text{Co}_2\text{Cl}$  and (1 0 1) as 17.99°, (1 1 1) as 20.12° and (0 0 2) as 28.56° for  $\text{HBO}_2$ . Reflections lines were present in the standard pattern of  $\text{Co}_2\text{Cl}$  and  $\text{HBO}_2$  in the current JCPDS database with accession number 01-089-3733 and 01-077-0425 [20]. An increase in the solid state reaction temperatures affected the crystalline structure of the product.

According to Cavaliere et al., Co and B based catalyst can be formed in two ways, as cobalt boride ( $\text{Co}_x\text{B}$ ) or cobalt–boron alloy (Co–B) [23]. Due to the nature of intermetallic compound/alloy it is still not clear what the structure of the product is. In addition, XRD analyses confirmed that cobalt boron structure is defined as amorphous with at least one broad peak centered at around 45° (Fig. 2d). These results show the crystallinity of the structure and also the formation of cobalt boron structure. Many previous studies have shown the characteristic peaks of amorphous cobalt–boron [23–27].

After the solid state reaction, a pyrophoric material was obtained that had not been exposed to air or oxidative atmosphere such that oxidation was not completed. The conversion of  $\text{Co}_x\text{B}$  structure to Co–O has not occurred [18].

As indicated by the XRD results, formation of Co/B accelerator was accompanied by an increase in the solid-state synthesis temperature. At low temperatures, the main phases were  $\text{CoCl}_2$  and  $\text{H}_3\text{BO}_3$  while Co/B structure did not form. According

**Table 2** Particle sizes of products obtained at different solid state reactions

Code	Solid state synthesis temperature (°C)	Average particle size (μm)	Min. particle size (μm)	Max. particle size (μm)
PR-1	58	8.79	2.7	19.51
PR-2	112	7.94	2.44	17.65
PR-3	158	6.83	2.26	17.46

**Table 3** Physical, and chemical properties of Co/B Accelerator

Crystal phase	Composition (molar ratio Co:B)	$S_{\text{BET}}$ ( $\text{m}^2 \text{g}^{-1}$ )	Average particle size ( $\mu\text{m}$ )
Amorphous	0.57	1.36	6.05

to the XRD analysis of both solid state synthesis products, Co/B complex structure was formed successfully according to the DTA analysis results. The Co/B accelerator structure did not contain metal and boron source. This result indicated that boron oxide could be used as boron source for preparing of Co/B accelerator for hydrolysis of  $\text{NaBH}_4$ .

Fig. 3 shows the SEM images at 1,000 and 20,000 magnification of the products that had been prepared at different solid state synthesis temperatures. According to the SEM images of products, the average particle size decreased with increasing synthesis temperature (Table 2).

As a result, Co/B accelerator was synthesized at 196 °C for 4 h using a solid-state reaction. Physical and chemical properties of Co/B accelerator were determined by ICP–OES, BET, and SEM analyses (Table 3). The empirical formula of solid state synthesis Co/B accelerator was  $\text{CoB}_2$  according to the ICP results.

#### Solid state reaction kinetics of Co/B as a catalytic/acidic accelerator

In this study, the Kissinger and Doyle non-isothermal kinetic models were used in order to calculate the kinetic parameters for solid state reactions according to the DTA analysis.

In the Kissinger model,  $T_m$  at different heating rates was determined from DTA curves with the assumption that weight loss at  $T_m$  is constant. In the Doyle model, values of  $\log\beta$  plotted against  $1/T_m$  gave straight lines for all heating rates. The  $E_a$  value was calculated from the slope of the kinetic curve (Fig. 4). Co–B formation was observed at 196 °C, which indicated the last solid reaction in the DTA plot. The activation energy was calculated as 95.87 kJ/mol from the Kissinger kinetic model and 100.51 kJ/mol from the Doyle kinetic model. Both kinetic models were applied to all solid state reactions and  $E_a$  values were calculated as shown Table 4.  $E_a$  values of the two models were almost the same yet the four solid state reaction  $E_a$  values were different from each other.

#### Hydrogen generation tests of Co/B as a catalytic/acidic accelerator

The hydrogen generation tests of  $\text{NaBH}_4$  were performed in a test system. For the kinetic investigation of Co/B accelerator, a variety of reaction medium temperature of 22, 40 and 60 °C were applied. For all reaction medium temperatures, the induction time was inconsiderable as reaction starts immediately. Linear regression was applied to the hydrogen generation data with % 100 conversion (Fig. 5).

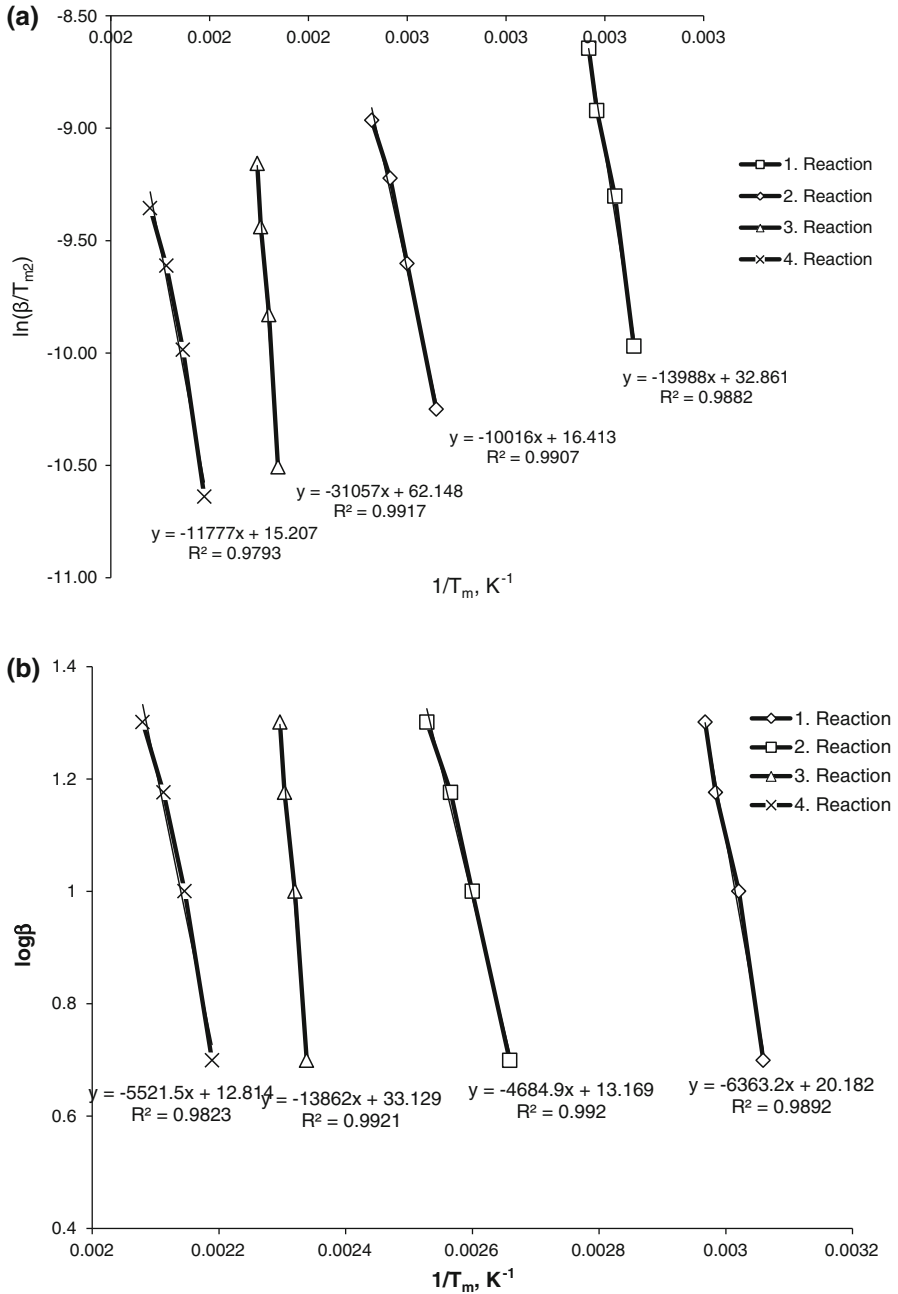


**Fig. 4** Kinetic plots of solid state reactions; **a** Kissinger model, **b** Doyle model

**Table 4** Reaction activation energies calculated by the Kissinger and Doyle methods

	Activation energy (kJ/mol)			
	$E_{a1}$	$E_{a2}$	$E_{a3}$	$E_{a4}$
Kissinger method	113.86	81.53	252.80	95.87
Doyle method	115.84	85.29	252.35	100.51

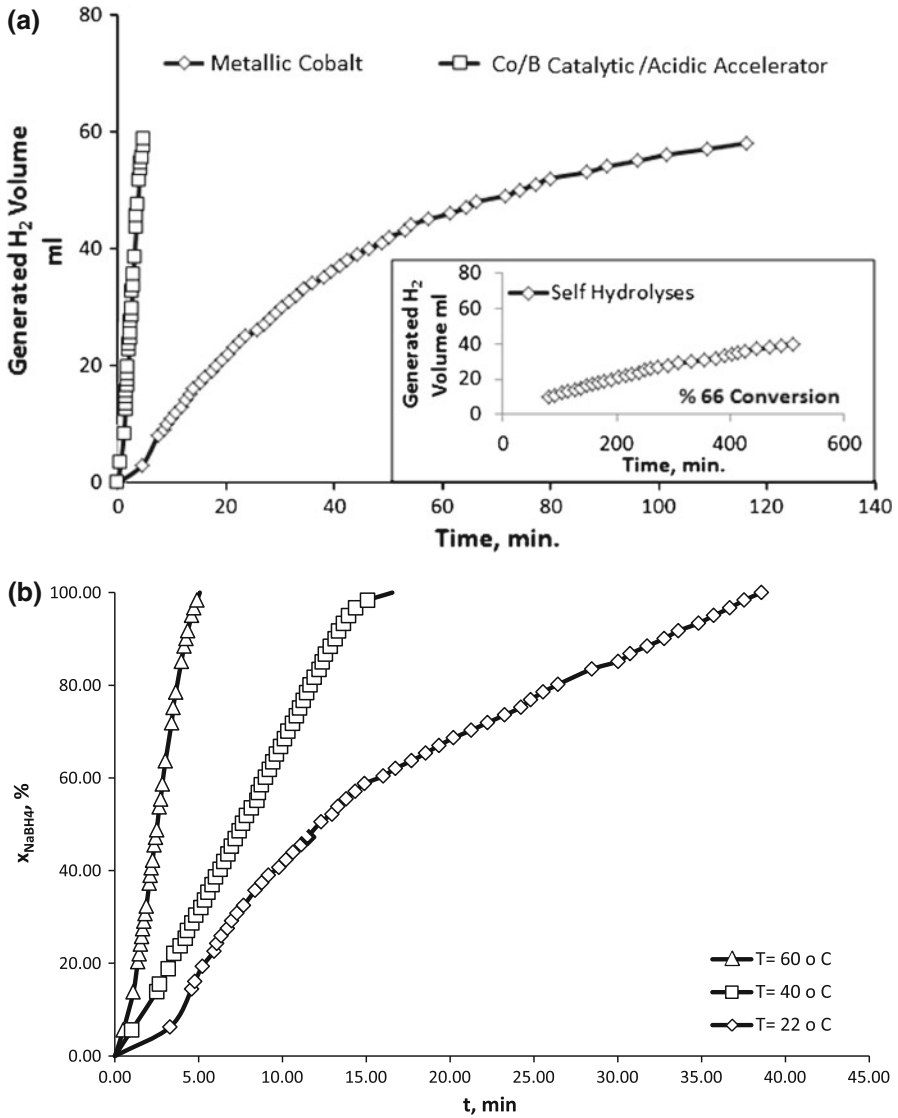


**Fig. 5** Hydrolysis data of NaBH<sub>4</sub> against time in the presence of: **a** metallic cobalt, Co/B catalytic/acidic accelerator and self-hydrolyses of NaBH<sub>4</sub> at 60 °C, **b** Co/B catalytic/acidic accelerator at different temperatures (22, 40, 60 °C)

After the characterization of the amorphous solid state synthesis of Co/B accelerator, it was used as a catalytic/acidic accelerator in the hydrolysis of  $\text{NaBH}_4$ .  $\text{H}_2$  generation versus time during  $\text{NaBH}_4$  hydrolysis over Co/B accelerator at a variety of temperatures (22, 40, and 60 °C). For the amorphous Co/B accelerator,  $\text{H}_2$  liberation followed a regular trend; an increase in the temperature led to faster  $\text{H}_2$  release. When the reacting temperature ranged from 22 to 60 °C, the reacting time declined from 38 to 3.5 min for amorphous Co/B accelerator.

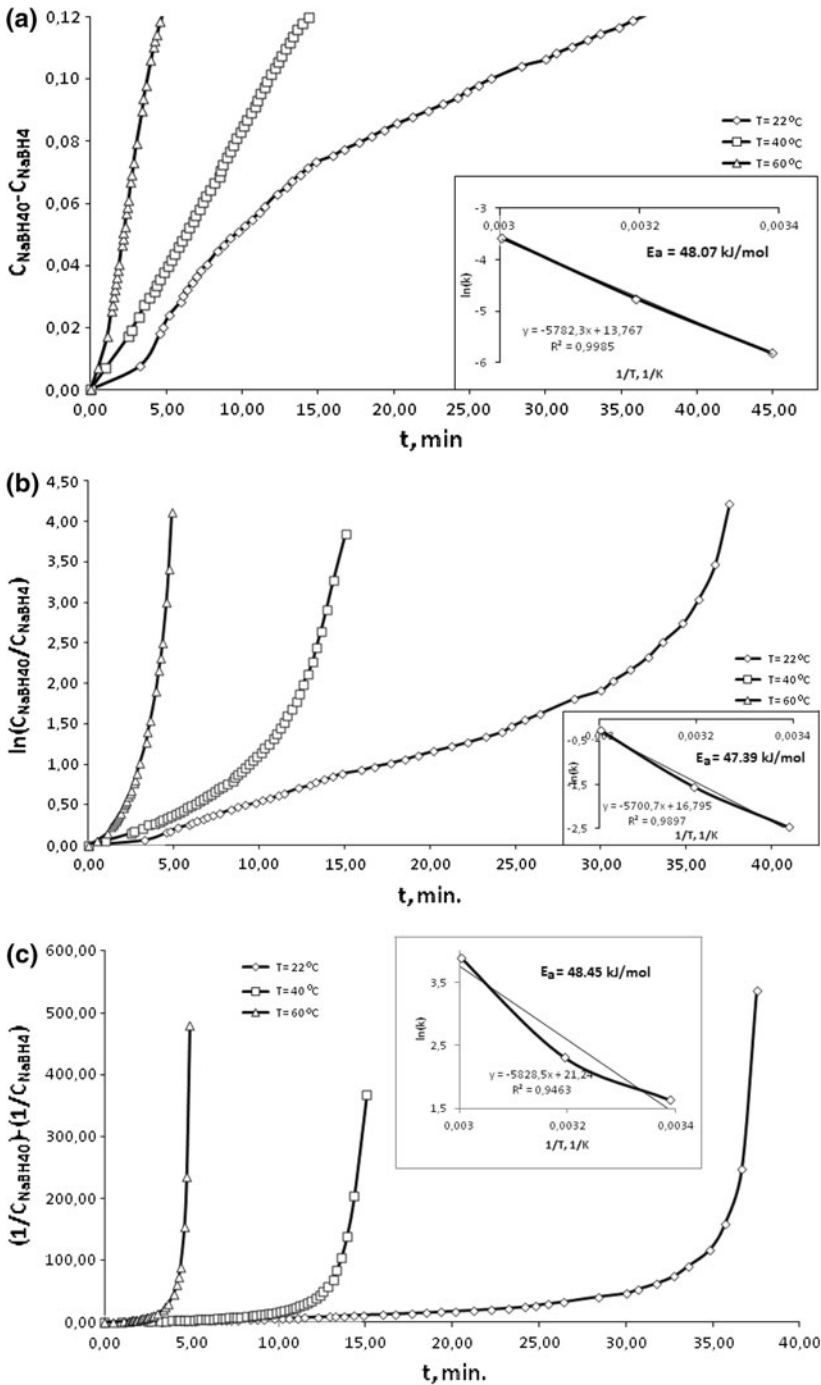
Table 5 shows  $\text{H}_2$  generation rates at different temperatures for amorphous Co/B accelerator. The hydrogen generation rate was determined from the linear portion of the plot for each temperature experiment. Time span values were taken into consideration in calculating  $\text{H}_2$  generation rate. The hydrogen generation rate increased with increasing temperature as expected. In the presence of 0.0025 g catalyst, the maximum  $\text{H}_2$  generation rate of 5,466.64  $\text{ml min}^{-1} \text{ g cat}^{-1}$  was observed at 60 °C for amorphous Co/B accelerator and whole reaction was finished in 3.5 min (Fig. 5).

Fig. 5a shows self  $\text{NaBH}_4$  hydrolysis and metallic cobalt catalyzed  $\text{NaBH}_4$  hydrolysis compare with Co/B accelerator catalyzed at 60 °C under 400 rpm magnetic stirring rate. Metallic cobalt can be used as a catalyst in  $\text{NaBH}_4$  hydrolyses.  $\text{NaBH}_4$  is a strong reducing agent and changes the activity of any cobalt and cobalt based catalyst. Thus, it is recommended that cobalt boride ( $\text{Co}_x\text{B}$ ) or cobalt–boron alloy (Co–B) is used instead of metallic cobalt. However, the absence or presence of various catalysts resulted in significant differences in hydrogen generation rates. The absence of catalyst in  $\text{NaBH}_4$  hydrolysis led to a very low hydrogen generation rate of about 0.0701  $\text{ml min}^{-1}$ , while metallic cobalt showed a hydrogen generation rate of only 0.5090  $\text{ml min}^{-1}$ . On the other hand, Co/B accelerator, synthesized by solid state reaction, led to 14.047  $\text{ml min}^{-1}$  hydrogen generation under the same conditions. Thus, the Co/B accelerator should be used instead of metallic cobalt to improve hydrogen generation. The most important feature is the necessity of the boron in the catalyst as it provides better activity. Boron modifies the electron density of cobalt and amorphous structure increases the active catalytic sites. For selected amorphous Co/B accelerator; zeroth, first and second order kinetic models were applied to determine the reaction characteristics; activation energy of the reaction was then calculated [23].

Fig. 6a shows that the zeroth order kinetic model for Co/B accelerator applied to the hydrolysis of  $\text{NaBH}_4$  calculated the activation energy as 48.07  $\text{kJ mol}^{-1}$  for amorphous Co/B accelerator with a good correlation coefficient of 0.9985. According to the linear regression calculations, the zeroth order kinetic model fit best to the reaction kinetics data. This means that the hydrolysis of  $\text{NaBH}_4$  in the

**Table 5**  $\text{H}_2$  generation rate at different temperatures for the amorphous Co/B Accelerator

Hydrolysis results	Temperature (°C)			Activation energy (kJ/mol)		
	22	40	60	Zeroth order	first order	Second order
$\text{H}_2$ generation rate ( $\text{ml H}_2 \text{ min}^{-1} \text{ g cat}^{-1}$ )	590.32	1,666.72	5,466.64	48.07	47.39	48.45



**Fig. 6** Kinetic plots of  $NaBH_4$  hydrolysis reactions in the presence of Co/B catalytic/acidic accelerator; **a** Zeroth order model, **b** First order model, and **c** Second order model

**Table 6** Activation energy in the presence of various catalysts from aqueous  $\text{NaBH}_4$ 

Catalyst	Preparation method	Activation energy ( $\text{kJ mol}^{-1}$ )	Ref.
CoB-amorphous	Chemical reduction	64.87	[5]
Co-B quasi amorphous	Chemical reduction	$55.20 \pm 1.70$	[12]
5 wt% Co- $\alpha\text{Al}_2\text{O}_3$	Impregnation	53.80	[16]
10 wt% Co- $\alpha\text{Al}_2\text{O}_3$	Impregnation	51.50	[16]
15 wt% Co- $\alpha\text{Al}_2\text{O}_3$	Impregnation	53.00	[16]
Ni-Co-B	Chemical reduction	62.00	[22]
Ru(5 wt%)/IRA-400	Chemical reduction	56.00	[6]
Ru/C	–	37.30	[24]
Metallic cobalt	–	75.00	[25]
Co/B Accelerator amorphous	Solid state	48.07	This study

presence of Co/B accelerator is independent of  $\text{NaBH}_4$  concentration. Fig. 6b shows the first order kinetic model for Co/B accelerator applied to the hydrolysis of  $\text{NaBH}_4$  calculated the activation energy as  $47.39 \text{ kJ mol}^{-1}$  for the amorphous Co/B accelerator with a correlation coefficient of 0.9897. Fig. 6c shows the second order kinetic model, which calculated the activation energy as  $48.45 \text{ kJ mol}^{-1}$  for amorphous Co/B accelerator with correlation coefficient of 0.9463.

These values compare favorably with the reported results for Co/B accelerator. The value of the  $E_a$  for Co/B accelerator ( $48.07 \text{ kJ mol}^{-1}$ ) was lower than the results for metallic cobalt ( $75 \text{ kJ mol}^{-1}$ ) [25], CoB-amorphous ( $64.87 \text{ kJ mol}^{-1}$ ) [5], Co-B quasi amorphous ( $55.20 \text{ kJ mol}^{-1}$ ) [12], and Ni-Co-B ( $62.00 \text{ kJ mol}^{-1}$ ) [22]. Table 6 provides a comparison of the value of  $E_a$  in this work with some other published values. It was seen that amorphous Co/B accelerator showed high catalytic activity and low cost for  $\text{H}_2$  generation from  $\text{NaBH}_4$ .

## Conclusion

In the present study, Co/B catalytic/acidic accelerator was prepared via solid state method for the first time. We recommended to synthesize catalytically active amorphous Co/B as a catalytic/acidic accelerator based on solid state method as an alternative to pelletization, chemical reduction and, impregnation methods. According to the investigation, the following points result from this study:

- The Co/B accelerator was prepared at a lower temperature of  $196 \text{ }^\circ\text{C}$ .
- For the solid state reaction, both non-isothermal kinetic models gave almost the same results for activation energies. The activation energy was calculated as  $95.87 \text{ kJ mol}^{-1}$  from the Kissinger kinetic model and  $100.51 \text{ kJ mol}^{-1}$  from the Doyle kinetic model.
- Maximum hydrogen generation rate was determined as  $5,466.64 \text{ ml H}_2 \text{ g cat}^{-1} \text{ min}^{-1}$  at  $60 \text{ }^\circ\text{C}$  in the presence of solid state prepared Co/B accelerator.



- Co/B as a catalytic/acidic accelerator should be used instead of metallic cobalt to improve hydrogen generation.
- The zeroth order kinetic model was found to give the best fit for amorphous Co/B accelerated hydrogen generation. The activation energy was calculated as  $48.07 \text{ kJ mol}^{-1}$  with 0.9985 as a correlation coefficient.

**Acknowledgments** The authors would like to thank the Yildiz Technical University Research Foundation (Project no: 2012-07-01-YL02) for its financial support. Technical assistance of UNIDO-ICHET for BET analysis is gratefully acknowledged.

## References

1. Yang CC, Chen MS, Chen YW (2011) Hydrogen generation by hydrolysis of sodium borohydride on CoB/SiO<sub>2</sub> catalyst. *Int J Hydrogen Energy* 36–2:1418–1423
2. Santos DMF, Sequeira CAC (2011) Sodium borohydride as a fuel for the future. *Renew Sustain Energy Rev* 15:3980–4001
3. Umegaki T, Yan JM, Zhang XB, Shioyama H, Kuriyama N, Xu Q (2009) Review boron- and nitrogen-based chemical hydrogen storage materials. *Int J Hydrogen Energy* 34:2303–2311
4. Liu CH, Wua YC, Chou CC, Chen BH, Hsueh CL, Ku JR, Tsau F (2012) Hydrogen generated from hydrolysis of ammonia borane using cobalt and ruthenium based catalysts. *Int J Hydrogen Energy* 37:2950–2959
5. Jeong SU, Kim RK, Cho EA, Kim H-J, Nam S-W, Oh I-H, Hong S-A, Kim SH (2005) A study on hydrogen generation from NaBH<sub>4</sub> solution using the high-performance B<sub>2</sub>O<sub>3</sub>-CoCl<sub>2</sub> powder. *J Power Sources* 144:129–134
6. Amendola SC, Sharp-Goldman SL, Janjua MS, Spencer NC, Kelly MT, Petillo PJ, Binder M (2000) A safe, portable, hydrogen gas generator using aqueous borohydride solution and Ru catalyst. *Int J Hydrogen Energy* 25:969–975
7. Retnamma R, Novais AQ, Rangel CM (2011) Kinetics of hydrolysis of sodium borohydride for hydrogen production in fuel cell applications: a review. *Int J Hydrogen Energy* 36:9772–9790
8. Akdim O, Demirci UB, Muller D, Miele P (2009) Cobalt(II) salts, performing materials for generating hydrogen from sodium borohydride. *Int J Hydrogen Energy* 34:2631–2637
9. Liang J, Li Y, Huang Y, Yang J, Tang H, Wei Z, Shen KP (2008) Sodium borohydride hydrolysis on highly efficient Co-B/Pd catalysts. *Int J Hydrogen Energy* 33:4048–4054
10. Akdim O, Demirci UB, Muller D, Miele P (2009) Cobalt(II) salts, performing materials for generating hydrogen from sodium borohydride. *Int J Hydrogen Energy* 34:2631–2637
11. Akdim O, Demirci UB, Muller D, Miele P (2009) More reactive cobalt chloride in the hydrolysis of sodium borohydride. *Int J Hydrogen Energy* 34:9444–9449
12. Delmas J, Laversenne L, Rougeaux I, Garron P, Garron A, Benicci S, Swierczynski D, Auroux A (2011) Improved hydrogen storage capacity through hydrolysis of solid NaBH<sub>4</sub> catalyzed with cobalt boride. *Int J Hydrogen Energy* 36:2145–2153
13. Jeonga SU, Chob EA, Namb SW, Ohb IH, Junga UH, Kima SH (2007) Effect of preparation method on Co-B catalytic activity for hydrogen generation from alkali NaBH<sub>4</sub> solution. *Int J Hydrogen Energy* 32:1749–1754
14. Liu BH, Li Q (2008) A highly active Co/B accelerator for hydrogen generation from sodium borohydride hydrolysis. *Int J Hydrogen Energy* 33:7385–7391
15. Lu Y-C, Chen M-S, Chen Y-W (2012) Hydrogen generation by sodium borohydride hydrolysis on nanosized CoB catalysts supported on TiO<sub>2</sub>, Al<sub>2</sub>O<sub>3</sub> and CeO<sub>2</sub>. *Int J Hydrogen Energy* 37:4254–4258
16. Chamoun R, Demirci UB, Zaatar Y, Khoury A, Miele P (2010) Co- $\alpha$ Al<sub>2</sub>O<sub>3</sub>-Cu as shaped catalyst in NaBH<sub>4</sub> hydrolysis. *Int J Hydrogen Energy* 35:6583–6591
17. Metin O, Kocak E, Ozkar S (2011) Effect of stabilizer type on the activity and stability of water-dispersible cobalt(0) nanocluster catalysts in hydrogen generation from the hydrolysis of sodium borohydride. *Reac Kinet Mech Cat* 103:325–340

18. Schlesinger HI, Brown ER, Finholitam AE, Gilbreathh JR, Hoekstra HR, Hyde EA (1953) Sodium borohydride, its hydrolysis and its use as a reducing agent and in the generation of hydrogen. *J Am Chem Soc* 75(1):215–219
19. Kantürk Figen A, Sarı Yılmaz M, Pişkin S (2010) Structural characterization and dehydration kinetics of Kırka inderite mineral: application of non-isothermal models. *Mater Charact* 61:640–647
20. Hung AJ, Tsai SF, Hsu YY, Ku JR, Chen YH, Yu CC (2008) Kinetics of sodium borohydride hydrolysis reaction for hydrogen generation. *Int J Hydrogen Energy* 33:6205–6215
21. Levenspiel O (1999) *Chemical Reaction Engineering*, 3rd edn. John Wiley & Sons, New York
22. Sevim F, Demir F, Bilen M, Okur H (2006) Kinetic analysis of thermal decomposition of boric acid from thermogravimetric data. *Korean J Chem Eng* 23(5):736–740
23. Cavaliere S, Hannauer J, Demirci UB, Akdim O, Miele P (2011) Ex situ characterization of  $N_2H_4$ -,  $NaBH_4$ - and  $NH_3BH_3$ -reduced cobalt catalysts used in  $NaBH_4$  hydrolysis. *Catal Today* 170(1):3–12
24. Krishnan P, Advani SG, Prasad AK (2008) Cobalt oxides as  $Co_2B$  catalyst precursors for the hydrolysis of sodium borohydride solutions to generate hydrogen for PEM fuel cells. *Int J Hydrogen Energy* 33(23):7095–7102
25. Fernandes R, Patel N, Miotello A (2009) Hydrogen generation by hydrolysis of alkaline  $NaBH_4$  solution with Cr-promoted Co–B amorphous catalyst. *Appl Catal B* 92:68–74
26. Feng Y, Jiao L, Yuan H, Zhao M (2007) Effects of amorphous CoB on the structural and electrochemical characteristics of MgNi alloy International. *Int J Hydrogen Energy* 32:2836–2842
27. Amendola SC, Sharp-Goldman SL, Janjua MS, Kelly MT, Petillo PJ, Binder M (2000) An ultrasafe hydrogen generator: aqueous, alkaline borohydride solutions and Ru catalyst. *J Power Sources* 85:186–189